Thermochimica Acta, 97 (1986) 313–320
Elsevier Science Publishers B.V., Amsterdam – Printed in The Netherlands

THERMAL STUDIES OF THE $CaCO_3$:SiO_2 (2:1) SYSTEM CONTAINING LITHIUM AS DOPANT

I.P. SARASWAT *, V.K. MATHUR ** and S.C. AHLUWALIA **

Department of Chemistry, University of Roorkee, Roorkee (U.P.) (India)

(Received 5 July 1985)

ABSTRACT

Li_2CO_3 dopant lowers the decomposition temperature of $CaCO_3$ and the process takes place in two steps. CaO formed at low temperature reacts with SiO_2 to form the β-dicalcium silicate (C_2S; C = CaO, S = SiO_2) phase even at 750°C. The reaction is completed at 1350°C, with the formation of β-C_2S and small amounts of γ-C_2S by the addition of 1% dopant. Addition of 5% dopant brings the final reaction temperature down to 1290°C, the reaction products being β-C_2S and small amounts of the tricalcium silicate (C_3S) phase.

INTRODUCTION

Studies on the kinetics and thermodynamic parameters of the decomposition of pure calcium carbonate and the effect of various dopants have been reported by several workers [1–6]. Work has also been done on the thermal dissociation of naturally occurring limestone containing cationic impurities [7–9]. A literature survey reveals that the systematic study of the 2:1 molar $CaCO_3$:SiO_2 system containing Li_2CO_3 as dopant has received virtually no attention. Some work with LiCl as mineralizer in the formation of C_2S [10] and of Li_2CO_3 as intensifier [11] in the 3:1 molar $CaCO_3$:SiO_2 mixture has been reported.

The present paper deals with the effect of varying amounts of Li_2CO_3 on the thermal behaviour of a mixture of $CaCO_3$:SiO_2 (2:1).

EXPERIMENTAL

Materials and sample preparation

To a mixture of reagent grade $CaCO_3$ and quartz powder (purity > 99.5%) in 2:1 molar ratio, varying amounts of Li_2CO_3 (calculated as 0.1–5% Li_2O)

* Author to whom all correspondence should be addressed.
** National Council for Cement and Building Materials, M-10 NDSE II, New Delhi, 110049, India.

0040-6031/86/$03.50

were added. The resulting mixture, after thorough mixing, grinding and passing through a 100-μm sieve, were shaped in the form of nodules with small amounts of distilled water. The samples, after drying at 100 ± 5°C for 2 h, were tested for quantitative estimation of $CaCO_3$ to ensure complete homogenization. These dried samples were stored for the experimental work.

Thermal analysis

The measurements were made on Mettler thermal analyser (TA-1), which simultaneously records the DTA, DTG and TG curves. In all cases, 60-mg samples were heated at a rate of 8°C min^{-1} in a platinum crucible of the thermal analyser. α-Al_2O_3 (previously burned to 1500°C for 30 min) was used as the reference material.

The activation energy (E_a) of $CaCO_3$ decomposition was calculated from the DTG curve by the methods given in ref. 12. The enthalpy (ΔH) and the shape index were determined from the DTA curve [13,14].

X-ray diffraction studies

The samples for analysis were powdered to pass through a 45-μm sieve and pressed into a sample holder. The instrument used was a Philips model PW 1120. The diffraction patterns were recorded using a copper target and nickel filter.

Examination of the intermediate phases indicated by DTA

Samples, in the form of nodules, were heated in a quench furnace at a rate of 8°C min^{-1} in a platinum bucket to the temperature at which the DTA peak ends, retained for 30 min at that temperature and immediately quenched in liquid nitrogen.

Estimation of free lime

The amount of free lime in the final products (obtained after heating at the final DTA peak temperature for 1 h) was estimated by titrating the ethylene glycol extract with standard HCl [15].

RESULTS AND DISCUSSION

The thermal behaviour of the system is shown in Fig. 1. The salient thermal features and the kinetic parameters (E_a, ΔH and shape index), calculated on the basis of major peaks, are given in Table 1. For comparison, the data for pure 2 : 1 molar $CaCO_3$ and SiO_2 mixtures are also given in this

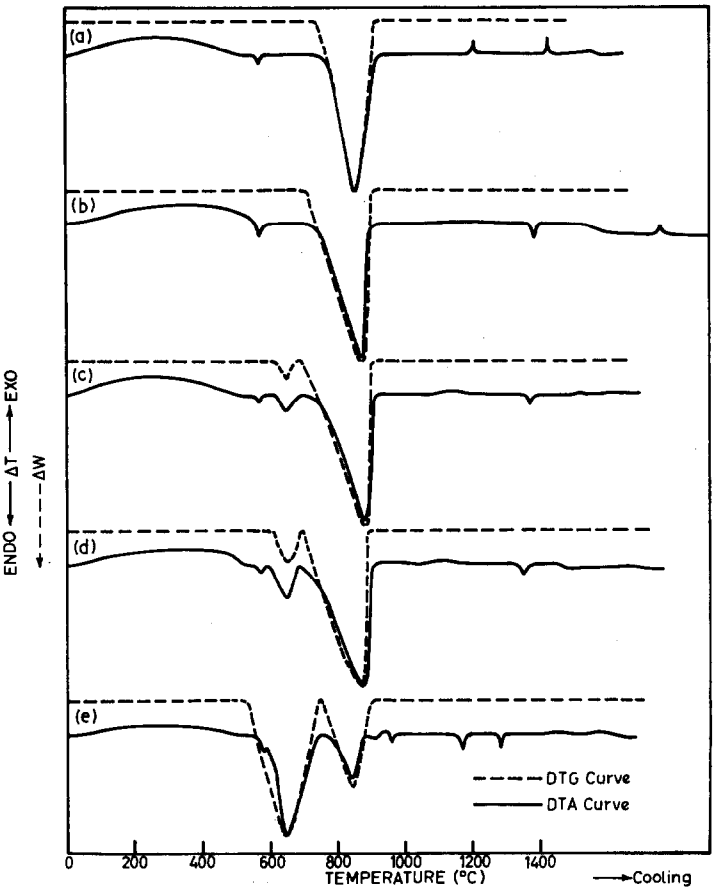

Fig. 1. Thermal curves of (a) $2CaCO_3:SiO_2$; (b) $2CaCO_3:SiO_2+0.1\%\ Li_2CO_3$; (c) $2CaCO_3:SiO_2+0.5\%\ Li_2CO_3$; (d) $2CaCO_3:SiO_2+1\%\ Li_2CO_3$; (e) $2CaCO_3:SiO_2+5\%\ Li_2CO_3$.

table. From the above, it is observed that for lithium carbonate dopant, calculated as 5% Li_2O, the behaviour is different from that of other concentrations of the dopant.

The thermal curves (DTG and DTA) having 0.1% Li_2CO_3 (0.1% Li_2O) did not show a separate peak for the decomposition of Li_2CO_3, due to its small mass. However, for the higher percentages of the dopant, the DTG and the DTA curves indicate that the decomposition takes place in two steps, i.e., the decomposition of Li_2CO_3 precedes that of $CaCO_3$. As the concentration of Li_2CO_3 changes through 0.5, 1 and 5%, approximately 2, 6 and 81% $CaCO_3$, respectively, undergoes decomposition along with all the Li_2CO_3 in the first step. No distinct peak for the decomposition of Li_2CO_3 alone is discerned for 5% dopant and an inflexion is observed in the early stages of the peak. It is observed (Table 1) that with the increase in the concentration of the dopant from 0.1 to 1%, the temperature of initial decomposition (T_i), the

TABLE 1

Thermal analysis data of $2CaCO_3 : SiO_2$ in the presence of Li_2CO_3

Sample	Decomposition of Li_2CO_3 and $CaCO_3$ from DTG and DTA curves (°C)						Enthalpy, ΔH, calculated from DTA (kJ mol^{-1})	Activation energy, E_a, calculated from DTG (kJ mol^{-1})	Shape index of 2nd peak	Final DTA peak after calcination of $CaCO_3$ (°C)	Phases observed by XRD
	First peak			Second peak							
	T_i	T_d	T_f	T_i	T_d	T_f					
$2CaCO_3 : SiO_2$ [19]	–	–	–	740	850	910	160	247	0.143	1425(exo)	β-C_2S, γ-C_2S, free lime
$2CaCO_3 : SiO_2$ + Li_2CO_3(0.1% Li_2O)	–	–	–	710	885	900	155	207	0.176	1390(endo)	γ-C_2S, β-C_2S, free lime (0.07%)
$2CaCO_3 : SiO_2$ + Li_2CO_3(0.5% Li_2O)	620	650	680	700	880	900	135	200	0.250	1370(endo)	γ-C_2S, β-C_2S, free lime (0.30%)
$2CaCO_3 : SiO_2$ + Li_2CO_3(1% Li_2O)	620	650	690	690	870	890	120	187	0.350	1350(endo)	β-C_2S, γ-C_2S, free lime (0.43%), Li_2CaSiO_4 (small amount)
$2CaCO_3 : SiO_2$ + Li_2CO_3(5% Li_2O)	540	650	740	740	850	890	126	245	0.430	1290(endo)	β-C_2S, C_3S, Li_2CaSiO_4, quartz, free lime (0.22%)

enthalpy (ΔH) and the activation energy (E_a) for the decomposition decrease but the temperature at which the decomposition peaks terminate (T_f), is not greatly affected. This trend of the thermodynamic parameters is not followed for 5% dopant. The behaviour is somewhat similar to that reported for the 2:1 $CaCO_3$:SiO_2 mixture containing varying amounts of alkaline earth dopants [16].

All the DTA curves show a distinct endotherm at 575°C due to α–β quartz transformation. This transformation temperature is not influenced by the dopant. The second endotherm appearing at the same DTG peak, $T_i = 620$°C and $T_f = 680$ and 690°C for 0.5 and 1% dopant, respectively, may be due to melting and complete decomposition of Li_2CO_3 along with partial decomposition of $CaCO_3$. In the literature, simultaneous melting and decomposition temperatures ranging from 712 to 728°C and polymorphic transformations at lower temperatures are reported [17,18]. It is well known that impurities bring down the decomposition temperature. The third endotherm could be assigned to the decomposition of the remaining $CaCO_3$ and formation of silicates.

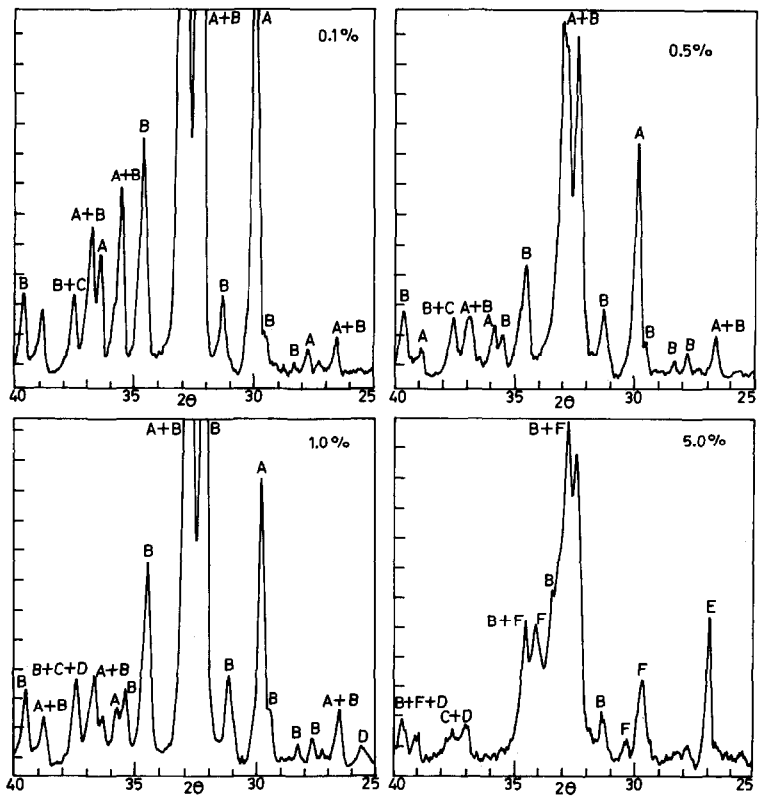

Fig. 2. XRD patterns of lithium-doped dicalcium silicate phase. (A) γ-C_2S, (B) β-C_2S, (C) free lime, (D) Li_2CaSiO_4, (E) quartz, (F) C_3S.

TABLE 2

Intermediate compounds formed at various endothermic DTA peaks as characterized by X-ray diffraction of liquid nitrogen-quenched samples of $2CaCO_3 : SiO_2 + 5\%$ Li_2CO_3 (as Li_2O)

Endothermic DTA peak at (°C)	Compounds formed at the end of the DTA peak	Corresponding most intense *d* values (Å)	Reported *d* values as per ASTM cards (JCPDS values) (Å)
650	Free time	2.40, 2.77, 1.70, 1.45	2.405, 2.77, 1.70, 1.45
	Quartz	4.27, 3.33, 2.45, 1.81	4.26, 3.34, 2.46, 1.81
	$CaCO_3$	3.56, 3.02, 2.80,	3.57, 3.02, 2.81
	Li_2SiO_3	4.68, 2.71, 2.34, 1.56	4.70, 2.71, 2.34, 1.57
	β-C_2S	2.80, 2.78, 2.74, 2.61	2.79, 2.78, 2.74, 2.608
850	Free lime	2.40, 2.77, 1.70, 1.45	2.40, 2.77, 1.70, 1.45
	Quartz	4.27, 3.33, 2.45, 1.81	4.27, 3.33, 2.45, 1.81
	$Li_2Si_2O_5$	3.61, 3.72, 2.40, 5.45	3.61, 3.73, 2.40, 5.45
	β-C_2S	2.80, 2.78, 2.74, 2.61	2.80, 2.78, 2.74, 2.61
	γ-C_2S	2.73, 2.75, 3.01, 3.82	2.73, 2.75, 3.00, 3.82
960	Free lime	2.40, 2.77, 1.70, 1.45	2.40, 2.77, 1.70, 1.45
	Quartz	4.27, 3.33, 2.45, 1.81	4.27, 3.33, 2.45, 1.81
	Li_2CaSiO_4	2.40, 3.58, 1.99	2.40, 3.58, 1.99
	β-C_2S	2.80, 2.78, 2.74, 2.61	2.80, 2.78, 2.74, 2.61
	γ-C_2S	2.73, 2.75, 3.01, 3.82	2.73, 2.75, 3.01, 3.82
1170	β-C_2S	2.80, 2.78, 2.74, 2.61	2.80, 2.78, 2.74, 2.61
	γ-C_2S	2.73, 2.75, 3.01, 3.82	2.73, 2.75, 3.01, 3.82
	Li_2CaSiO_4	2.40, 3.58, 1.99	2.40, 3.58, 1.99
	Free lime	2.80, 2.78, 2.74, 2.61	2.80, 2.78, 2.74, 2.61
	Quartz	4.27, 3.33, 2.45, 1.81	4.27, 3.33, 2.45, 1.81

Surprisingly, after the decomposition endotherm no exotherm is observed. This behaviour is in sharp contrast with that of alkaline earth carbonate dopants [19]. The various phases that are formed at the end of the final DTA peak temperature are given in Table 1. These were identified from the XRD patterns (Fig. 2).

These thermal effects become quite prominent for 5% dopant concentration. Therefore, the phases present in the liquid nitrogen-quenched sample at the end of each endotherm have been examined by XRD. The details are given in Table 2.

At 750°C, not only complete decomposition of Li_2CO_3 and partial decomposition of $CaCO_3$ takes place, but detectable amounts of β-C_2S and Li_2SiO_3 are also formed. This might be due to the greater activity of CaO and Li_2O formed at lower temperatures. In the sample quenched at 880°C, Li_2SiO_3 changes to $Li_2Si_2O_5$, more β-C_2S is formed, along with some γ-C_2S. Free lime and quartz are also present between 880 and 980°C, a small endotherm at 960°C is preceded by a broad, weak inflexion. The inflexion may be due to the melting of $Li_2Si_2O_5$ [20]. As a result of this, the XRD

lines in the sample quenched at 980°C are broadened with the overlapping of peaks, perhaps due to the formation of a solid solution and metastable phases. A few new low-intensity lines appear in the XRD (maybe due to solid solution formation), which are not identifiable from the ASTM cards. Low-intensity lines are observed for β-C_2S, γ-C_2S, free lime and Li_2CaSiO_4 (lithium calcium silicate). At 1200°C, the sharp lines of β-C_2S, γ-C_2S, quartz and Li_2CaSiO_4 appear along with some C_3S phase and free lime. At 1300°C, the XRD pattern of the liquid nitrogen-quenched sample predominantly indicates β-C_2S, some C_3S, quartz and very small amounts of Li_2CaSiO_4. This might be due to the substitution of Li^+ for Ca^{2+} and Si^{4+} and its incorporation in the interstitial sites of C_3S, which is quite possible, since tetrahedrally coordinated Li^+ is well established in many compounds [21].

The absence of γ-C_2S might be due to its partial conversion into β-C_2S and disproportionation of that remaining to C_3S according to the following equation:

$$3C_2S(\gamma\text{-form}) = 2C_3S + S$$

This not only explains the formation of C_3S but also the increased amounts of β-C_2S and quartz in the final product.

Plots of the ratio of β-C_2S and γ-C_2S (XRD line intensity ratios have been used) vs. concentration of the dopants show that the amount of γ-C_2S progressively decreases with the increase in the concentration of the dopant, until, finally, it is not observed for 5% dopant (Fig. 3a). A plot of free lime vs. dopant concentration shows an upward trend initially (up to 1% dopant) and drops from 0.43 to 0.22% for 5% dopant. This drop is attributed to some of the free lime reacting to form C_3S (Fig. 3b).

The shape index (Table 1) of the DTA peak for $CaCO_3$ decomposition

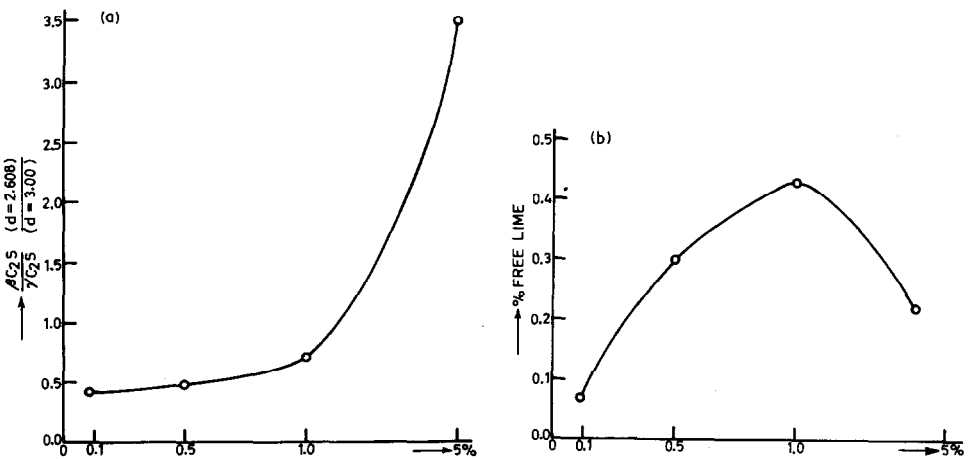

Fig. 3. (a) Effect of dopant on the ratio of β-/γ-C_2S phase (XRD line intensity ratio has been used). (b) Concentration of dopant vs. free lime.

indicates that, with increasing dopant concentration, the kinetics of reaction approach unity.

CONCLUSIONS

(1) Li_2CO_3 dopant lowers the decomposition temperature of $CaCO_3$ and causes the decomposition to take place in two steps.

(2) CaO formed at lower temperature is very reactive and reacts with SiO_2 to form β-C_2S even at 750°C.

(3) As the concentration of the dopant increases from 0.1 to 5%, the amount of β-C_2S increases progressively and its formation temperature decreases from 1425°C (without any dopant) to 1300°C. Further, the amounts of free lime also increase with increasing dopant concentration and some C_3S is also formed with 5% dopant.

(4) Li_2CO_3 (calculated as 1% Li_2O) appears to be quite effective as an intensifier.

ACKNOWLEDGEMENT

The authors are thankful to Dr. H.C. Visvesvaraya, Chairman and Director General, National Council for Cement and Building Materials, New Delhi for providing research facilities for the pursual of Ph.D. studies to one of the authors (V.K.M.).

REFERENCES

1 H. Lehmann and M. Schmidt, Tonind. Ztg., 85 (1961) 73.
2 G.V. Subbarao, M. Natrajan and C.N.R. Rao, J. Am. Ceram. Soc., 51 (1968) 179.
3 B.D. Chattaraj, S.N. Dutta and M.S. Iyer, J. Therm. Anal., 5 (1973) 43.
4 P.K. Gallagher and D.W. Thonson, Thermochim. Acta, 14 (1976) 255.
5 C.R.M. Rao and P.N. Mehrotra, Indian J. Chem., 15A (1977) 1016.
6 S.N. Ghosh, A.K. Paul and A.K. Thakur, J. Mater. Sci., 13 (1978) 1602.
7 A.K. Gupta, M. Rai, Chem. Age India, 28 (1977) 199.
8 W.U. Malik, D.R. Gupta, H.O. Gupta and R.S. Gupta, Indian Ceram., 25 (1982) 63.
9 I. Masood, N.G. Dave and R.S. Gupta, Indian Ceram., 25 (1982) 83.
10 A. Packter and M.A.S. Zaidi, Silikattechnik, 27 (1976) 14.
11 O. Korab, Z. Hrabe and J. Ryba, Zb. Pr. Chemickotechnol. Fak. SVST, 6 (1972) 301.
12 N.G. Dave and S.K. Chopra, Z. Phys. Chem., Neue Folge, 48 (1966) 256.
13 D.M. Speros and R.L. Woodhouse, J. Phys. Chem., 72 (1968) 2846.
14 H.E. Kissinger, Anal. Chem., 29 (1957) 1702.
15 M.P. Javellana and I. Jawed, Cem. Concr. Res., 12 (1982) 399.
16 I.P. Saraswat, V.K. Mathur and S.C. Ahluwalia, Thermochim. Acta, 87 (1985) 37.
17 N.N. Semenov and T.V. Zabolotskii, Izv. Sib. Otd. Akad. Nauk SSSR, 2 (1962) 58.
18 Otsubo and K. Yamaguchi, J. Chem. Soc. Jpn., 82 (1961) 557.
19 I.P. Saraswat, V.K. Mathur and S.C. Ahluwalia, Thermochim. Acta, 95 (1985) 201.
20 F.P. Glasser, Phys. Chem. Glasses, 8 (1967) 224.
21 E. Woermann, Th. Hahn and W. Eysel, Cem. Concr. Res., 9 (1979) 701.